ANALYSIS OF STARS COMMON TO THE *IRAS* AND *HIPPARCOS* SURVEYS

Timothy G. Knauer,[1] Željko Ivezić,[2] and G. R. Knapp[2]
Received 2000 July 21; accepted 2001 January 16

ABSTRACT

For about 11,000 stars observed in the *Hipparcos* Survey and detected by *IRAS*, we calculate bolometric luminosities by integrating their spectral energy distributions from the B band to far-IR wavelengths. We present an analysis of the dependence of dust emission on spectral type and of the correlations between luminosity and dust emission for about 1000 sources with the best data (parallax error less than 30%; luminosity error $\sim 50\%$ or better). This subsample includes stars of all spectral types and is dominated by K and M giants. We use the *IRAS* $[25]-[12]$ color to select stars with emission from circumstellar dust and show that they are found throughout the Hertzsprung-Russell diagram, including on the main sequence. Clear evidence is found that M giants with dust emission have luminosities about 3 times larger ($\sim 3000 \ L_{\odot}$) than their counterparts without dust and that mass loss on the asymptotic giant branch for both M and C stars requires a minimum luminosity of order 2000 $L_{\odot}$. Above this threshold the mass-loss rate seems to be independent of, or only weakly dependent on, luminosity. We also show that the mass-loss rate for these stars is larger than the core-mass growth rate, indicating that their evolution is dominated by mass loss.

Subject headings: circumstellar matter — infrared: stars — stars: AGB and post-AGB —
stars: fundamental parameters — stars: mass loss — surveys

On-line material: color figures

1. INTRODUCTION

Dust can be found around pre–main-sequence, main-sequence, and post–main-sequence stars (e.g., Zuckerman 1980; Habing 1996; Waters & Waelkens 1998). The relationships between the luminosity of a star, its evolutionary phase, and the properties of its circumstellar dust are not fully understood. The main obstacle is the lack of a large uniform sample which would include both dust emission properties and the stellar luminosity and spectral type. In this paper we present such a sample of stars for which these quantities are obtained by combining the results of *Infrared Astronomical Satellite* (*IRAS*) and *High Precision Parallax Collecting Satellite* (*Hipparcos*) surveys. While there have been studies correlating *IRAS* data with data from other catalogs (e.g., with the SAO catalog; Oudmaijer et al. 1992), the determination of luminosity for a large number of stars has become possible only recently owing to the release of the *Hipparcos* astrometric data.

IRAS produced a survey of 96% of the sky at 12, 25, 60, and 100 μm, with the resulting *IRAS* Point Source Catalog (PSC) containing over 250,000 sources. The colors based on *IRAS* fluxes can efficiently be used to distinguish pre–main-sequence from post–main-sequence stars and to study characteristics of the dust emission (e.g., van der Veen & Habing 1987; Ivezić & Elitzur 2000, hereafter IE00). The recently released *Hipparcos* catalog contains parallaxes of unprecedented accuracy for 118,218 sources and is complete to $V \sim 7.5$ (Perryman et al. 1997). Combining these two data sets can yield bolometric luminosities for a large number of stars and facilitate studies of the relationship between the characteristics of dust emission and stellar luminosity.

In § 2 we describe a catalog of stars obtained by positionally matching the *IRAS* and *Hipparcos* catalogs. For 11,321 matched sources, we calculate bolometric fluxes by integrating their spectral energy distributions (SEDs) from the B band to far-IR wavelengths and bolometric luminosities with the aid of *Hipparcos* parallaxes. In § 3, we present an analysis of the dependence of dust emission on spectral type and correlations between the luminosity and dust emission for 968 sources with the most accurate luminosities (standard deviation of $\sim 50\%$ or better), and in § 4 we discuss the relationship between mass loss and luminosity for asymptotic giant branch (AGB) stars.

2. THE SYNTHESIS OF THE *IRAS* POINT SOURCE AND *HIPPARCOS* CATALOGS

We consider only sources from the *IRAS* Point Source Catalog (PSC) with quality flags of at least 2 in at least two *IRAS* bands.[3] This is motivated by the results described by IE00, who showed that dusty stars come in two "flavors": AGB stars, which typically have fluxes in the 12 and 25 μm bands larger than the fluxes in the 60 and 100 μm bands, and various young stellar objects with fluxes in the 60 and 100 μm bands larger than the fluxes in the 12 and 25 μm bands. There are 88,619 sources with high-quality fluxes in the 12 and 25 μm bands and 33,435 sources with high-quality fluxes in the 60 and 100 μm bands. We note that the number of sources with good fluxes at only 25 and 60 μm is very small compared to the above (3612, or less than 3%), in agreement with IE00.

The quoted *IRAS* positional 2 σ error ellipse for stars is typically $3'' \times 20''$, and its position angle varies across the sky (Beichman et al. 1988). However, the typical distance between *Hipparcos* sources (about 30') is much larger than the *IRAS* error ellipse, and we simply match the positions of

[1] Department of Physics and Astronomy, University of Kentucky, Lexington, KY 40506-0055; knauer@pop.uky.edu.
[2] Department of Astrophysical Sciences, Princeton University, Princeton, NJ 08544-1001; ivezic@astro.princeton.edu, gk@astro.princeton.edu.

[3] The reliability of an *IRAS* flux is described by the quality index: 3 is high, 2 is low, 1 is an upper limit.
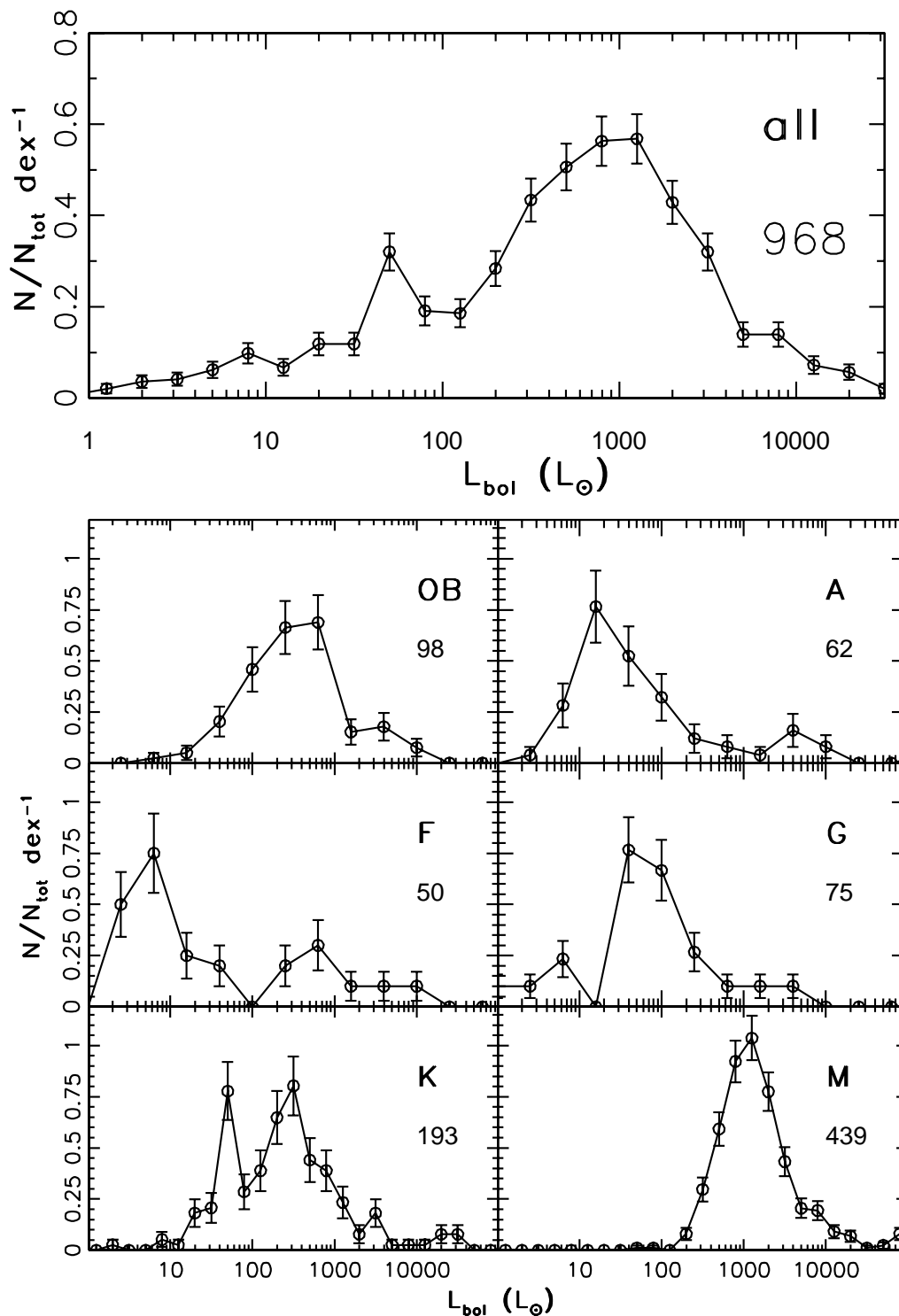
FIG. 1.—Luminosity histogram for 968 stars with most reliable luminosity estimates (see text). Top panel shows the distribution for all stars irrespective of spectral type; six lower panels detail the same information separated by spectral type. All luminosity classes are included. Number of stars in each spectral type subsample is given below the spectral type designation in each panel.

stars within a circle of radius 25″. This matching radius ensures that practically all true matches are included while keeping the random association rate below ~5 × 10⁻⁴. Also, this radius is sufficiently small that the number of *Hipparcos* sources matched with multiple *IRAS* sources is negligible (there are only four such cases for which we took the closer match). The positional correlation of the subset of ~125,666 *IRAS* sources with the full *Hipparcos* catalog resulted in 11,321 matches. The positional discrepancies are consistent with the mean *IRAS* error of ~10″. From the random association rate we estimate that about 50 matched sources (0.4% of the sample) are random associations.[4] We

---

[4] This number could be decreased by about a factor of 2 by explicitly treating the *IRAS* error ellipse information, but this does not seem necessary since the contamination is already negligible.
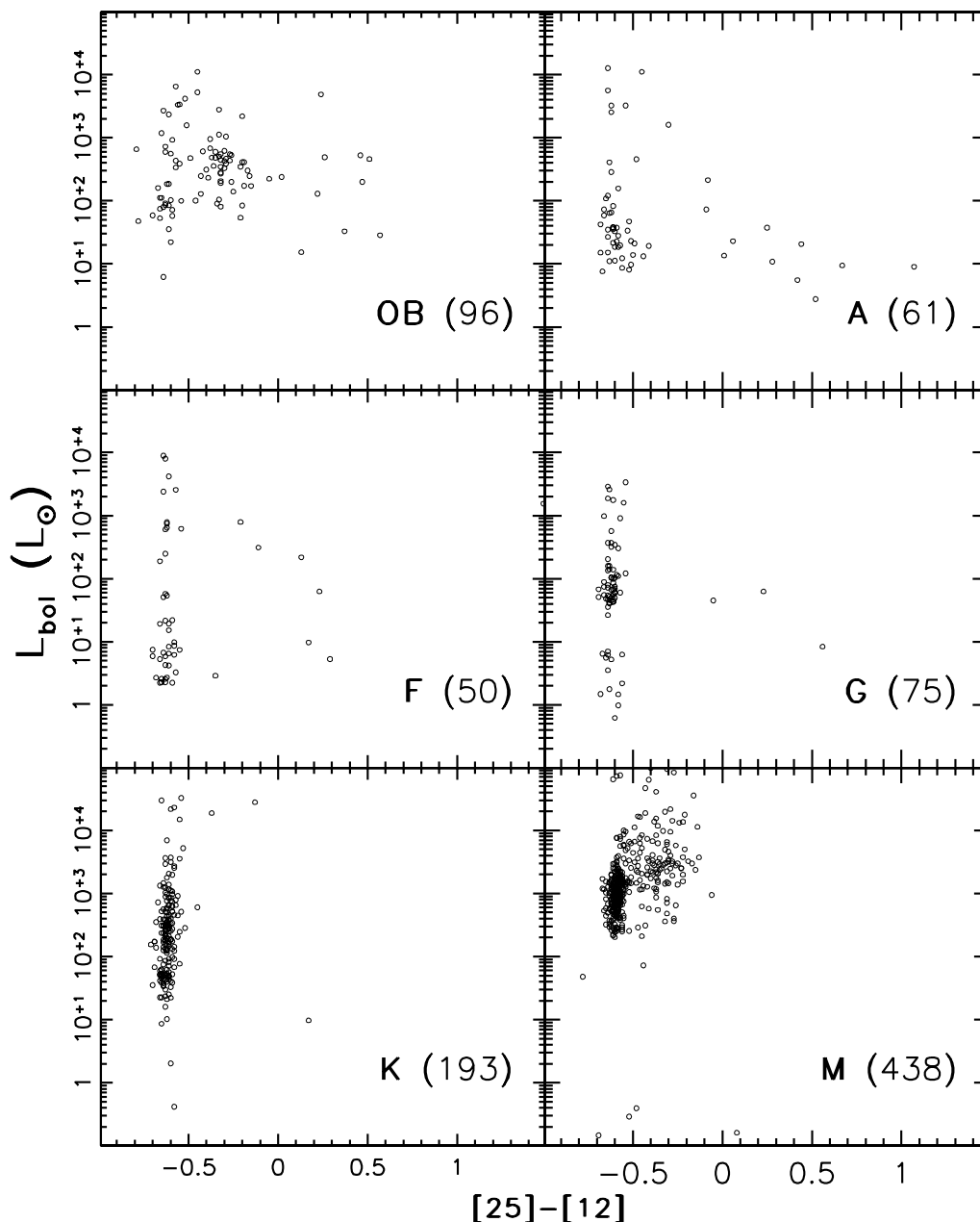
F‌IG. 2.—Bolometric luminosity vs. [25] − [12] diagram for 913 stars (*dotted*) from Fig. 1, which have *IRAS* flux qualities at 12 and 25 μm of at least two and have known spectral types. Panels show different spectral types, as marked.

estimate the completeness of our matched sample by increasing the matching radius to 45″, which produces 11,853 matches. Taking into account the increase in the expected number of random associations, this implies that our adopted sample includes ∼95% of all true *Hipparcos-IRAS* associations.

As expected, the matched sources are predominantly red *Hipparcos* stars, and the majority satisfy $0.9 < B−V < 1.6$ and $V < 9$. When considering the *IRAS* catalog, 77% of sources matched in the *Hipparcos* catalog are dust-free stars (see § 3) brighter than 1 Jy at 12 μm. The faint limit for the matched dust-free stars with "blue" SEDs is imposed by the *IRAS* sensitivity. The faint cutoff for matched dusty stars (approximately 2 times brighter than the cutoff for the input *IRAS* sample) with "red" SEDs is imposed by the *Hipparcos* sensitivity. Because of this cutoff, the matching of

the *Hipparcos* catalog to a deeper IR catalog, e.g., *IRAS* Faint Source Catalog, would not significantly increase the sample of dusty stars with good distance estimate.

For all matched stars we calculate bolometric fluxes by integrating their SEDs from the *B* band to the *IRAS* 100 μm band. We use photometric measurements provided by the *Hipparcos* main catalog and from the Catalog of Infrared Observations (CIO), which consists of inputs from other catalogs and observations culled from the literature, beginning in 1965 (Gezari et al. 1993). The number of flux measurements per star ranges from six to ∼20 with a median value of 10. We have used two integration methods: linear interpolation in log (λ)–log (flux) space and piecewise fitting of the Planck curve. The two methods typically agree within 20%–30%. From the piecewise fitting of the Planck curve to the endpoint pairs we estimate the flux outside the observed
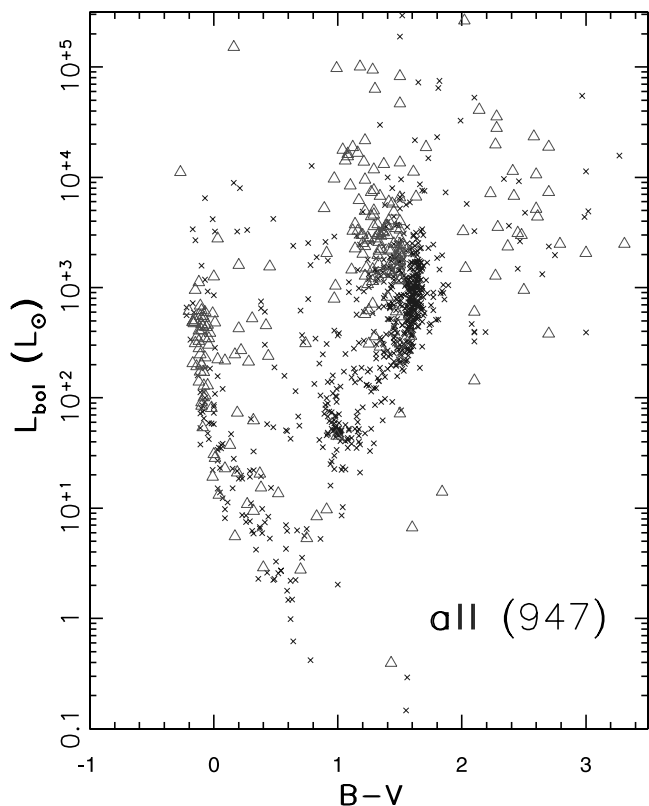
FIG. 3.—Bolometric luminosity vs. $B-V$ diagram for 947 stars from Fig. 1 with $V < 11$ mag. *Triangles*: $[25]-[12] > -0.5$. *Crosses*: $[25]-[12] < -0.5$. [*See the electronic edition of the Journal for a color version of this figure.*]

wavelength range to be typically less than 10%. From the bolometric fluxes and *Hipparcos* parallaxes we calculate bolometric luminosities for all 11,321 stars.[5]

Figure 1 displays the luminosity histogram for a subsample of matched stars with maximum fractional error in parallax of 30% and at least nine fluxes used for the bolometric flux calculation (968 stars). Relaxing the parallax cutoff to 50% roughly doubles the sample size but noticeably increases the number of outliers in various diagrams to be discussed later. The top panel in Figure 1 shows the distribution for all stars, irrespective of spectral type.[6] The error bars are assigned assuming a Poisson error distribution. There are two obvious peaks at ~ 50 $L_\odot$ and ~ 1000 $L_\odot$. The six panels below detail the same information separated by spectral type; all luminosity classes are included. Since there are so few O and B stars in the sample, they are treated together. The numbers of stars in each spectral type subsample, given below the spectral type designation in each panel, show that the sample is dominated by K and M giants. The comparison of the histogram for the full sample (*top panel*) to the various spectral subsamples shows that the peak at ~ 50 $L_\odot$ is due to K subgiants, also known as the red clump stars (for a detailed discussion, see Oudmaijer et al. 1992), and that the peak at

~ 1000 $L_\odot$ is due to M giants (note that the *Hipparcos* magnitude limit detects M dwarfs only out to 5 pc).

From the width of the peak for K stars at ~ 50 $L_\odot$, we estimate an upper limit on the mean L_bol error of $\sim 50\%$ (were this error larger, this peak could not be so narrow). Assuming that *Hipparcos* parallaxes and our method for determining bolometric fluxes are not biased with respect to spectral type, we adopt this value as the mean L_bol error for the whole sample. However, we note that dusty stars with heavily reddened SEDs may have large errors owing to sparse IR photometry, and the error distribution in such a case would be markedly non-Gaussian.

3. THE RELATIONSHIP BETWEEN LUMINOSITY AND SPECTRAL PROPERTIES

Figure 2 shows L_bol versus $[25]-[12]$ color[7] for 913 stars from Figure 1, with *IRAS* flux qualities of at least two at 12 and 25 μm and known spectral types. Color temperature increases from right to left, and $[25]-[12] = -0.6$ corresponds to the Rayleigh-Jeans tail of the Planck function. Stars with this color have no dust, and the distribution width indicates the errors in the *IRAS* fluxes ($\lesssim 10\%$). Stars with $[25]-[12] \gtrsim -0.5$ emit more IR radiation than a pure blackbody; this excess is usually attributed to dust emission (however, the IR excess for some O and B stars may be dominated by free-free emission). A significant fraction ($\sim 60\%$) of B and A stars show such IR excess and are probably young pre–main-sequence stars (Herbig Ae/Be stars; Waters & Waelkens 1998). A few F and G stars with IR excess are probably post–asymptotic giant branch stars (Oudmaijer et al. 1992). The M stars are shown in the lower right panel and are further discussed in § 4. However, it can already be seen in this diagram that M stars with dust are typically more luminous than those without dust. Note also that early-type stars (OBA) with IR excess have much redder $[25]-[12]$ colors (up to ~ 1) than M stars with IR excess ($\lesssim 0$). This difference is due to different dust density distributions in the circumstellar envelopes which are flatter for early-type stars than for late-type stars (IE00).

Figure 2 shows that stars with mid-IR excess can be simply selected as those with $[25]-[12] > -0.5$. Figure 3 displays L_bol versus $B-V$ diagrams for a subsample of 947 stars satisfying $V < 11$ mag, with (239) and without (708) IR excess, marked by triangles and crosses, respectively. It is easily discernible that dusty stars are found throughout the Hertzsprung-Russell diagram. The three dominant dusty populations are early-type OBA stars with $L_\mathrm{bol} \gtrsim 10$ $L_\odot$ and $B-V \lesssim 0.6$, and two types of late-type stars (further discussed in § 4) with $L_\mathrm{bol} \sim 10^3$–10^4 $L_\odot$: M stars with $B-V \sim 1.3$ and carbon stars with $B-V \gtrsim 2.0$ (Wallerstein & Knapp 1998).

4. DUST AROUND ASYMPTOTIC GIANT BRANCH STARS

Asymptotic giant branch stars are intermediate-mass stars in a late evolutionary stage just preceding the planetary nebula phase. Owing to copious mass loss (up to several 10^{-4} $M_\odot$ yr^{-1}), they are surrounded by dusty shells which emit distinctive IR radiation (for an extensive review, see Habing 1996). It is not clear what the relationship is between the mass-loss rate and luminosity for AGB stars.

---

[5] We ignore the correction for interstellar extinction since the sample is dominated by nearby stars ($\lesssim 300$ pc).

[6] The histogram counts are expressed as normalized counts per unit log interval (dex^{-1}); that is, the integrals of the plotted curves over $d(\log L_\mathrm{bol})$ are unity.

[7] We define *IRAS* $[25]-[12]$ color as $\log (F_{25}/F_{12})$, where F_{12} and F_{25} are the flux densities taken from the *IRAS* PSC.

Early studies by Gilman (1972) and Salpeter (1974) and later studies by others (e.g., Netzer & Elitzur 1993; Habing, Tignon, & Tielens 1994) showed that the luminosity-to-mass ratios for AGB stars are sufficiently large that mass loss could be driven by radiation pressure. Furthermore, Ivezić & Elitzur (1995, hereafter IE95) find that steady state radiation-pressure driven outflow models can explain *IRAS* colors for at least 95% of AGB stars. However, in these models both the mass-loss rate and the stellar luminosity are free parameters and cannot be independently constrained from the observations. We use the available luminosity and IR colors for the sample of M giants discussed here to study this relationship.

The top panel in Figure 4 shows the bolometric luminosity versus $[25]-[12]$ color diagram for a subsample of 307 M stars with distances less than 300 pc. The luminosities of 255 stars without dust emission ($[25]-[12] < -0.5$) cluster around $L_{bol} \sim 1000\ L_\odot$, while 52 stars with dust emission have luminosities on average ~ 3 times larger. Only 5% of stars without dust emission have $L_{bol} > 3000\ L_\odot$, and only 13% of stars with dust emission have $L_{bol} < 1000\ L_\odot$. This difference in bolometric luminosity distributions is better seen in histograms shown in the bottom panel, which are plotted separately for each
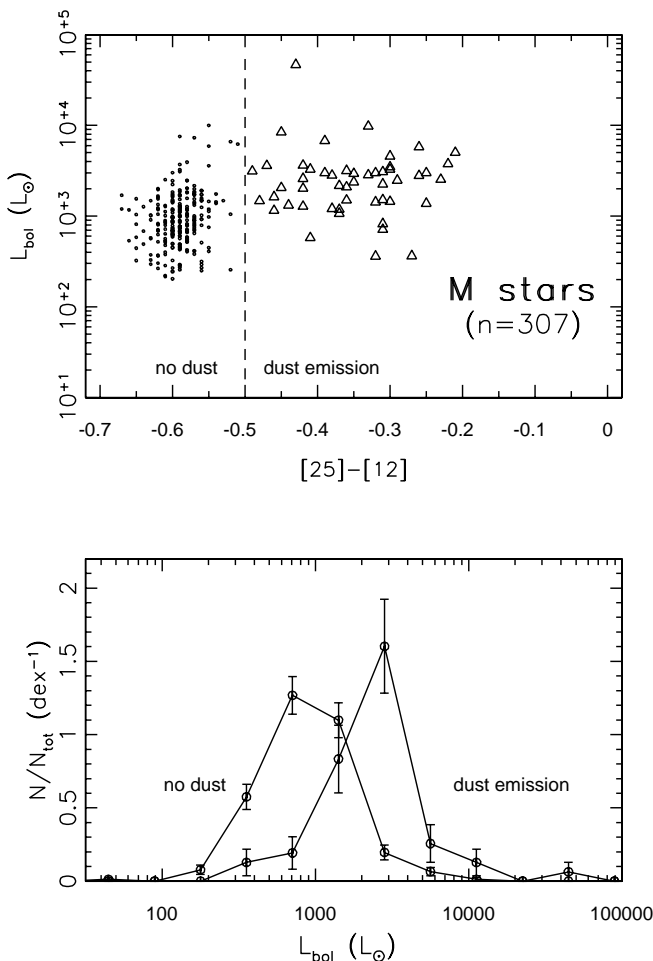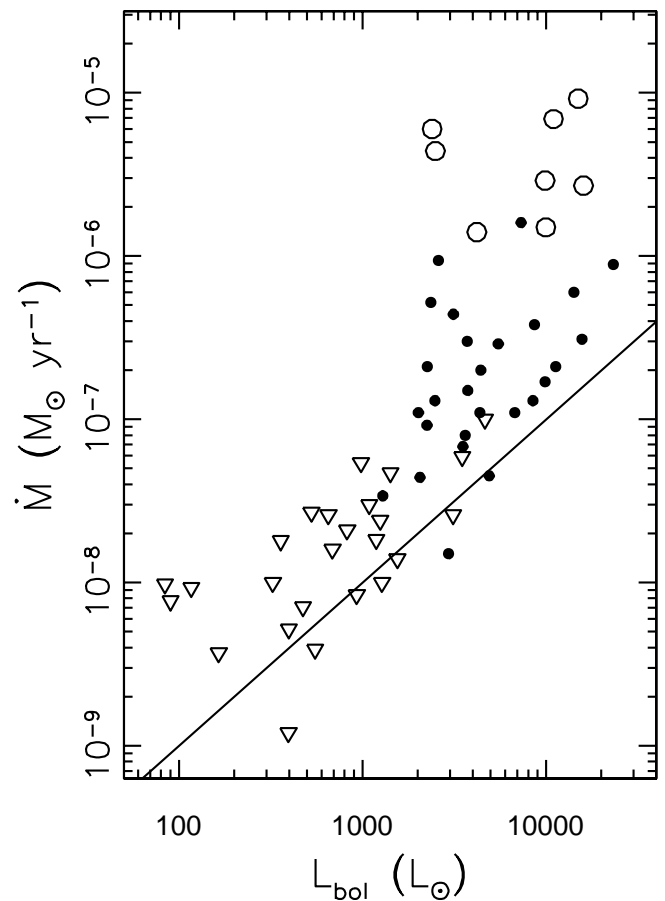
FIG. 5.—Mass-loss rate vs. bolometric luminosity for C stars (various symbols correspond to different methods for estimating mass-loss rate and distance; see text). The line indicates the core-mass growth rate. [*See the electronic edition of the Journal for a color version of this figure.*]

subsample. Figure 4 indicates that there is a characteristic luminosity of order 2000 $L_\odot$ for stars to develop a dusty envelope. Above this value the luminosity does not seem to be correlated with $[25]-[12]$ color, and its median luminosity for dusty M stars is $\sim 3000\ L_\odot$.

The scatter of points for dusty M stars around the median luminosity is somewhat larger than the expected errors derived in § 3 and thus may be real. However, the procedure used to determine bolometric flux is expected to be less accurate for stars emitting mostly in the IR because of sparse flux sampling. The method employed here for estimating bolometric flux can be significantly improved by utilizing detailed radiative transfer models for stars embedded in dusty envelopes. When fitting a model to the observed fluxes, the model SED acts as a smooth interpolating function, which produces a more robust estimate of the bolometric flux than an arbitrary function such as a piecewise power law (the bolometric flux is simply a scaling parameter; see Ivezić & Elitzur 1997). Such a detailed model fitting of a large number of sources will be presented in a separate publication.

The difference in median luminosities of stars with and without dust emission could be due to biased selection procedure. For example, if somehow dusty stars with $L_{bol} \lesssim 1000\ L_\odot$ are excluded from the sample, then the median luminosity of the remaining subsample is overestimated. We have tested our sample for this and similar pos-

FIG. 4.—*Top panel*: bolometric luminosity vs. $[25]-[12]$ diagram for 307 M giants with distances less than 300 pc. *Bottom panel*: luminosity histogram for nondusty vs. dusty M giants, as implied by their $[25]-[12]$ color. [*See the electronic edition of the Journal for a color version of this figure.*]

sibilities by relaxing the constraints on parallax, parallax error, V, and F_{12}, both individually and in various combinations. We find that the difference in median luminosity between the two subsamples is robust, even when the relaxed selection cuts result in a 3 times larger sample. Of course, in this case the scatter in luminosity around the median values is also increased, and we find that such outliers are mostly stars with relatively large parallax errors. Most notably, changing the distance cutoff from 200 pc to 500 pc does not effect the median luminosities of the two subsamples.

The median luminosity for dusty M stars obtained here (3000 $L_\odot$) is remarkably similar to the luminosity of AGB stars detected toward the Galactic bulge ($\sim 2600\ L_\odot$), as determined by Habing et al. (1985). This strongly suggests that the luminosity of AGB stars is roughly the same throughout the Galaxy and is also the same for stars with different mass-loss rates (the stars discussed by Habing et al. [1985] are significantly redder at $IRAS$ wavelengths than the stars discussed here that were selected from optical catalogs).

It is of interest to find out whether the luminosity versus mass-loss rate relation found for M stars also holds for AGB stars with carbonaceous dust grains. Due to different optical properties of silicate and carbonaceous grains, these stars do not show a large increase of [25]−[12] color for plausible mass-loss rates (IE95), and thus their mass-loss rate cannot be inferred from their [25]−[12] color. Nevertheless, the mass-loss rate for C stars can be determined from the intensity of their CO emission, and we utilize such observations to study the relationship between the mass-loss rate and bolometric luminosity for AGB stars with carbonaceous dust grains.

Figure 5 shows the mass-loss rate versus bolometric luminosity for a sample of 60 C stars with available CO emission observations (Knapp 2001). Distances are from the *Hipparcos* catalog for stars marked as filled circles and indirectly determined (Knapp 2001) for stars marked by open circles. The mass-loss rate for stars not detected in CO, marked by triangles, is determined from their $IRAS$ 60 μm fluxes as described in Jura (1991). The distribution of sources shows that for C stars there seems to be a threshold luminosity of the order 2000 $L_\odot$ for stars to develop a dusty envelope. Similarly to the result found for M stars, above this threshold the luminosity does not seem to be correlated with mass-loss rate. This threshold luminosity of about 2000 $L_\odot$ is in agreement with the theoretical estimate expected for radiatively driven winds (e.g., Ivezić, Knapp, & Elitzur 1998, and references therein).

Figure 5 also shows a line corresponding to

$$\dot{M}_{\mathrm{core}} = \frac{L_{\mathrm{bol}}}{0.007c^2},\qquad (1)$$

the approximate rate at which the inert helium core is growing from hydrogen shell burning (Schönberner 1983). At all luminosities the mass-loss rate is larger than the core-mass growth rate, indicating that mass loss dominates the evolution of these stars, in agreement with Wallerstein & Knapp (1998). Assuming the [25]−[12] color to mass-loss rate transformation as given by IE95, we find that the same conclusion also holds for M stars (cf. Fig. 4).

REFERENCES

Beichman, C. A., Neugebauer, G., Habing, H. J., Clegg, P. E., & Chester, T. J. 1988, *Infrared Astronomical Satellite (IRAS) Catalogs and Atlases. Volume 1: Explanatory Supplement* (Washington, DC: US GPO)
Gezari, D. Y., Schmitz, M., Pitts, P. S., & Mead, J. M. 1993, Catalog of Infrared Observations (NASA RP-1294; 3d ed.; Washington: NASA)
Gilman, R. C. 1972, ApJ, 178, 423
Habing, H. 1996, A&A Rev., 7, 97
Habing, H., et al. 1985, A&A, 152, L1
Habing, H. J., Tignon, J., & Tielens, A. G. G. M. 1994, A&A, 286, 523
Ivezić, Ž., & Elitzur, M. 1995, ApJ, 445, 415 (IE95)
———. 1997, MNRAS, 287, 799
———. 2000, ApJ, 534, L93 (IE00)
Ivezić, Ž., Knapp, G. R., & Elitzur M. 1998, in Sixth Annual CFD Conf. Proc. (Québec: CFD), IV-13

Jura, M. 1991, A&A Rev., 2, 227
Knapp, G. R. 2001, ApJ, submitted
Netzer, N., & Elitzur, M. 1993, ApJ, 410, 701
Oudmaijer, R. D., et al. 1992, A&AS, 96, 625
Perryman, M. A. C., et al. 1997, A&A, 323, L49
Salpeter, E. E. 1974, ApJ, 193, 579
Schönberner, D. 1983, ApJ, 272, 708
van der Veen, W. E. C. J., & Habing, H. J. 1988, A&A, 194, 125
Wallerstein, G., & Knapp, G. R. 1998, ARA&A, 36, 369
Waters, L. B. F. M., & Waelkens, C. 1998, ARA&A, 36, 233
Zuckerman, B. 1980, ARA&A, 18, 263